JHEP01(2014)115

Mixing stops at the LHC

Prateek Agrawal and Claudia Frugiuele

Fermilab,
P.O. Box 500, Batavia, IL 60510, U.S.A.

E-mail: prateek@fnal.gov, claudiaf@fnal.gov

ABSTRACT: We study the phenomenology of a light stop NLSP in the presence of large mixing with either the first or the second generation. R-symmetric models provide a prime setting for this scenario, but our discussion also applies to the MSSM when a significant amount of mixing can be accommodated. In our framework the dominant stop decay is through the flavor violating mode into a light jet and the LSP in an extended region of parameter space. There are currently no limits from ATLAS and CMS in this region. We emulate shape-based hadronic SUSY searches for this topology, and find that they have potential sensitivity. If the extension of these analyses to this region is robust, we find that these searches can set strong exclusion limits on light stops. If not, then the flavor violating decay mode is challenging and may represent a blind spot in stop searches even at 13 TeV. Thus, an experimental investigation of this scenario is well motivated.

Contents

1 Introduction

With the discovery of the particle consistent with standard model (SM) Higgs boson [1, 2], the hierarchy problem takes on a concrete and immediate nature. Low energy supersymmetry is one of the most studied and robust solutions to the hierarchy problem. A simple realization of supersymmetry is the Minimal Supersymmetric Standard Model (MSSM), which in its most general form suffers from a very acute flavor problem [3, 4]. The tension between flavor and natural low energy SUSY can be economically solved in models which predict spectra with degenerate squarks (and sleptons). In the pre-LHC era this paradigm provided a compelling framework of flavor in low energy SUSY models. However, the LHC bounds on these models push the spectrum of new states to the TeV scale, already requiring the SM to suffer some amount of fine-tuning.

Natural SUSY models surviving the LHC bounds now require a non-trivial flavor structure for the squark mass matrix so as to produce a hierarchical spectrum with the first and the second generation significantly heavier than the third generation [5, 6]. In the MSSM the structure of possible squark mass matrices is severely restricted by low energy observables [7–10]. R-symmetric models provide a compelling setting for investigating more complicated flavor structures since they generically admit larger mixing among the

squarks than in the MSSM [11]. This is a consequence of the fact that most flavor violating observables turn out to be proportional to terms which break R-symmetry, and are hence suppressed [11–13]. Therefore, a significant amount of flavor mixing is possible and quite generic. This could be an interesting ingredient in building flavorful SUSY breaking/mediation models, and also significantly alter the LHC signatures of SUSY particles [14].

Models with an (approximate) R-symmetry [11, 15–18] are additionally interesting as an alternative to the MSSM since they require the gauginos to be Dirac fermions.[1] This makes them less minimal than the MSSM in terms of the particle content, adding adjoint superfields for each SM gauge group, but on the other hand the Dirac character of the gauginos (particularly gluinos) can significantly soften the LHC exclusion limits on direct squark production [19–21]. Moreover, Dirac gluinos above the TeV scale are natural [22], while Majorana gluinos above that scale begin to saturate the naturalness threshold [5, 23]. This is a particularly interesting feature in light of the LHC limits on gluinos, $\sim 1.5\,\mathrm{TeV}$ [24].

In this paper we will investigate the implications of large flavor mixing for the LHC stop phenomenology. R-symmetric models provide an optimal setting for this scenario, but our discussion also applies to the MSSM when a significant amount of mixing can be accommodated. We will focus on a light stop NLSP (Next-to-Lightest Supersymmetric Particle) with a mass splitting $\Delta M = m_{\tilde{t}} - m_{LSP} \lesssim 250\,\mathrm{GeV}$ with the LSP. In this region of parameter space the mixing induced decays $\tilde{t} \to j + \mathrm{LSP}$ dominate, and hence completely alter the phenomenology of the stop.

The paper is organized as follows: we briefly review the main features of models with an approximate R-symmetry. We then present the effect of large flavor mixing on squark decays, focusing on the stop. The rest of the paper is devoted to the collider phenomenology of this scenario, with emphasis on the region of parameter space where the flavor violating decays dominate.

2 Mixed stops in R-symmetric models

One of the main features of R-symmetric models is that gauginos are Dirac fermions instead of Majorana. The R-symmetry also forbids A terms, which implies that there is no left-right mixing. Further, the μ-term is also not allowed. The combination of these features relaxes the SUSY flavor problem, allowing for a larger flavor violation both in the squark and in slepton sector than in the MSSM (see [11] and [13]). For instance, models with Dirac gluinos contribute to meson mixing through dimension 6 operators which are hence suppressed relative to the dimension 5 operators present in models with Majorana gluinos allowing for a potentially large mixing. The imaginary part of the $K - \bar{K}$ mixing is severely constrained by the measurement of ϵ_K. Therefore, the mixing in the first and second generation requires mild flavor structure in order to be consistent with the limits.

---

[1]The R-symmetry cannot be an exact symmetry since it is at least broken by the gravitino mass. The effects of the R-breaking are therefore communicated to the visible sector through anomaly mediation, see [11].

Flavor changing processes like $\mu \to e\gamma$ or $b \to s\gamma$ require a helicity flip in the corresponding diagrams which typically would arise from either a Majorana mass insertion, left right mixing between the squarks or a μ-term insertion in the large $\tan\beta$ limit; all these terms are forbidden by the R-symmetry. Therefore, one is left with a mass insertion in the external line which is significantly smaller, leading to the suppression of all the $\Delta F = 1$ processes. The R-symmetry also protects from dangerous contributions to $\Delta F = 1$ processes like $b \to s\gamma$ arising from a light stop. Moreover, the dangerous one-loop contributions to EDMs are forbidden by the R-symmetry since they all require either a Majorana mass insertion or squark left-right mixing.

The R-symmetry does not completely solve the flavor puzzle in SUSY. A mild flavor structure (in particular, a small phase) is still needed in order to satisfy the bounds from $K - \bar{K}$ mixing. However, many flavor violating observables are absent, and others significantly suppressed. Importantly, these suppressions are obtained independent of the SUSY breaking/mediation paradigm (beyond the requirement of R-symmetry). Therefore, the set of flavor assumptions for a viable R-symmetric SUSY model is much smaller than in the MSSM. Some more details on the flavor constraints are presented in appendix B.

In this work we are interested in exploring the consequences of having large flavor mixing on the stop phenomenology. As a simplifying assumption we only consider mixing between the second or the first generation and the third generation squarks, both in the left handed and in the right handed sector. We assume the unmixed generation to be heavy. Qualitatively our results continue to hold for more general flavor structures.

The state responsible for canceling the top quadratic divergence is the "33" state in the squark mass matrix $M_{\tilde{q}}^2$. Therefore, naturalness requirements affect $(M_{\tilde{q}}^2)_{33}$, which we choose to be $\lesssim (400\,\mathrm{GeV})^2$. In presence of flavor mixing $(M_{\tilde{q}}^2)_{33}$ is not the physical mass of the (mostly) stop squark, but is related to the two mixed squarks masses by the following relation:

$$(M_{\tilde{q}}^2)_{33} = \cos\theta^2 m_{\tilde{t}}^2 + \sin\theta^2 m_{\tilde{j}}^2 \tag{2.1}$$

where $\tilde{j}$ is either a (mostly) charm or up squark. The Higgs mass parameter thus becomes sensitive to the potentially heavier squark mass scale through the mixing. Therefore, the stop mass is not a robust measure of fine tuning in this scenario, and the fine tuning is in general worse than that deduced from the stop mass. The estimation of fine tuning then involves both the mixed generations. This is beyond the scope of this paper, and in the following we will assume the other generations to be above $650\,\mathrm{GeV}$ making them safe from the LHC bounds on three degenerate squarks (flavor-mixed partners of $\tilde{t}_R$ and $\tilde{t}_L$). This limit can be derived by rescaling the bounds on 8 degenerate squarks with decoupled gluinos. As shown in figure 1, this spectrum is still compatible with naturalness $((M_{\tilde{q}}^2)_{33} < (400\,\mathrm{GeV})^2)$.

It is also important to note that the presence of a large mixing angle can potentially affect the production cross section of stops at the LHC, since they can be now produced via their mixing with the charm or up-quark [25]. However, for sufficiently heavy (Dirac) gluinos we can assume this to be a subdominant effect, especially for the case when the stop mixes with the charm. Having heavy gluinos also means that the only source of squarks production at the LHC (at 7-8 TeV) is direct $\tilde{q}^*\tilde{q}$ production.
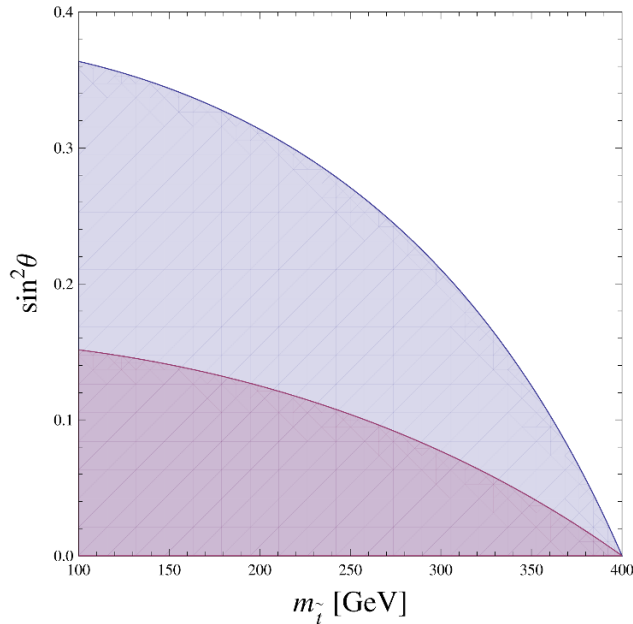
Figure 1. Natural region, which is chosen to be correspond to $(M_{\tilde{q}})_{33} < 400\,\text{GeV}$, for $m_{\tilde{j}} = 650\,\text{GeV}$ (light purple) and $m_{\tilde{j}} = 1\,\text{TeV}$ (darker purple).

3 Flavor violating stop decay modes

In this section we discuss the impact of large squark mixing in the third generation phenomenology, focusing on the NLSP stop scenario. This first requires us to specify the nature of the LSP. Third generation final states are preferred if the LSP contains an appreciable Higgsino component. This means that the flavor violating decays dominate for the first and second generation squarks, while the third generation phenomenology is not affected by the mixing. In this work, we focus on the case where the coupling is flavor universal, and the LSP is a pure bino neutralino or a gravitino.[2] The gravitino is often the LSP in R-symmetric models since its mass is related to the amount of R-breaking communicated to the visible sector through anomaly mediation [11]. Alternatively, a pure bino LSP is a good dark matter candidate. It is a pseudo-Dirac fermion, which means it annihilates more efficiently than the Majorana bino leading to the correct relic density in a large region of the parameter space [26]. On the other hand at the present day the pseudo-Dirac bino behaves like a Majorana fermion making it safe from direct detection constraints [27, 28]. We now discuss the phenomenology of a light stop $m_{\tilde{t}} < 400\,\text{GeV}$ for these two scenarios. For this purpose it is useful to separately discuss two regions: $m_{\tilde{t}} > m_t + m_{LSP}$ and $m_{\tilde{t}} < m_t + m_{LSP}$.

3.1 $m_{\tilde{t}} > m_t + m_{LSP}$

In this region of the parameter space a stop decays either into a t+LSP or j+ LSP where the jet is either a charm or up type jet (for large θ_{23} or θ_{13} respectively, denoted θ in the

---

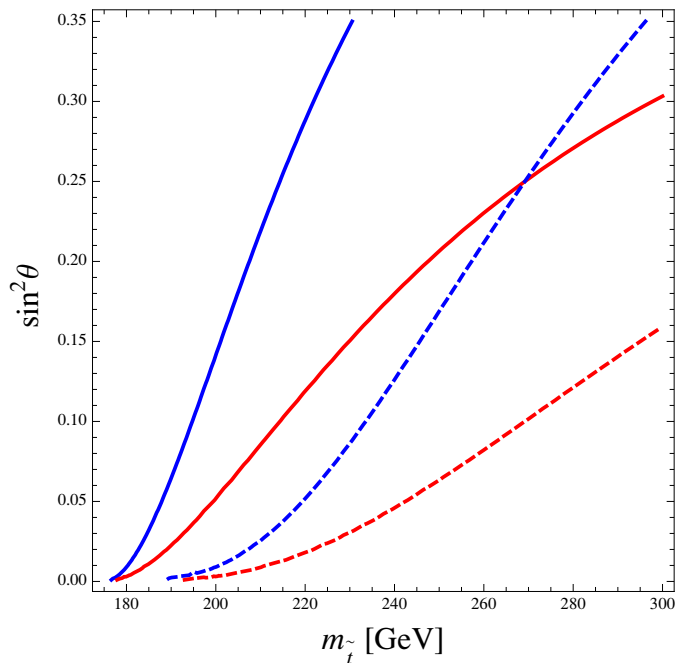[2]We do not consider a wino LSP since it typically implies light charginos, which are not the focus of our study.

Figure 2. Contour plot for the branching ratio $Br(\tilde{t} \to \tilde{B} + j)$ (solid) and $\mathrm{Br}(\tilde{t} \to G + j)$ (dashed) as function of the stop mass and the mixing. Contours are shown for branching ratio 75 % (blue) and 50% (red). The LSP is taken to be massless in both cases.

following). For a sufficiently heavy stop the branching ratio for the decay mode into light jet is $\sin^2\theta$, but in the almost degenerate region $m_{\tilde{t}} \sim m_t + m_{LSP}$ it gets enhanced due to the phase space suppression of the decay into top quarks, and hence could become the dominant decay mode. For instance, for a massless bino LSP the branching ratio for these decay modes are:

$$Br(\tilde{t} \to j\tilde{B}) = \frac{\sin^2\theta}{\sin^2\theta + \cos^2\theta\left(1 - \frac{m_t^2}{m_{\tilde{t}}^2}\right)^2}, \tag{3.1}$$

$$Br(\tilde{t} \to t\tilde{B}) = \frac{\cos^2\theta\left(1 - \frac{m_t^2}{m_{\tilde{t}}^2}\right)^2}{\sin^2\theta + \cos^2\theta\left(1 - \frac{m_t^2}{m_{\tilde{t}}^2}\right)^2}, \tag{3.2}$$

and for a massless gravitino LSP:

$$Br(\tilde{t} \to jG) = \frac{\sin^2\theta}{\sin^2\theta + \cos^2\theta\left(1 - \frac{m_t^2}{m_{\tilde{t}}^2}\right)^4}, \tag{3.3}$$

$$Br(\tilde{t} \to tG) = \frac{\cos^2\theta\left(1 - \frac{m_t^2}{m_{\tilde{t}}^2}\right)^4}{\sin^2\theta + \cos^2\theta\left(1 - \frac{m_t^2}{m_{\tilde{t}}^4}\right)^4}. \tag{3.4}$$

These equations apply for decays of both $\tilde{t}_L$ and $\tilde{t}_R$.

As shown in figure 2 the FV decay mode dominates over t+LSP for mass splitting $\Delta M \sim m_t$ due to the large mixing angle and phase space suppression. For a mixing of $\sin^2 \theta = 0.25$ the FV has order one branching ratio for stop masses up to $250\,\mathrm{GeV}$ for a massless bino LSP. For the gravitino this mode continues to dominate for much smaller mixing angles. Therefore, the FV mode is significant up to masses where dedicated searches for the topology t+LSP starts to be sensitive.

This is interesting since the region $m_t < m_{\tilde{t}} < 250\,\mathrm{GeV}$ represents an important lack of coverage of LHC analyses. Indeed the sensitivity of all the stop dedicated searches in the channel t plus LSP starts at 230-250 GeV both for ATLAS [29] and CMS [30] for a massless LSP. The challenge here is in distinguishing a possible stop signal over the top background. Due to the experimental difficulties this region ($m_{\tilde{t}} \sim m_t$) is called the stealth stop region [31]. For proposed dedicated searches in this region see [32, 33]. Alternatively, one can hope to discover the stealth stop relying on a different decay mode. In the MSSM when the stop is the NLSP the only other possible decay mode is into an off shell top and the LSP. However, the branching ratio for this three-body decay ends abruptly at $m_{\tilde{t}} = m_t$ for a neutralino LSP. If the gravitino is the LSP instead the branching ratio for three-body decay is significant ($\sim 20\%$) up to $200\,\mathrm{GeV}$, so the stealthy region is less broad [31]. We have shown that in our scenario, if the mixing is significant, a stop almost degenerate with the top quark will decay mostly into a light jet plus LSP. This can simplify the challenge of looking for stops into the stealth region. We will discuss this in the next section.

For heavier stops, $m_{\tilde{t}} \gg m_t + m_{LSP}$, the branching ratio for the decay mode into light jet is still large, but subdominant (it is proportional to $\sin^2 \theta$). As discussed in [34] this can potentially relax the bounds on the stops from the t LSP searches, [29] and [30]. Another interesting phenomenological implication of a significant squark mixing is single top production at the LHC ($pp \to \tilde{t}^*\tilde{t}$ with $\tilde{t} \to j$+LSP and $\tilde{t}^* \to t^*$+ LSP and vice versa). This topology constitutes a "smoking gun" signature for scenarios with a large squark mixing and it has been discussed in [34] and more extensively in [14]. It is important to note that the CMS and ATLAS analysis do not have a dedicated analysis for this mixed decay topology despite the low SM background.

3.2 $\quad m_{\tilde{t}} < m_t + m_{LSP}$

The two-body flavor conserving stop decays are forbidden for $m_{\tilde{t}} < m_t + m_{LSP}$. We will show that, for sufficiently large mixing angle, the two-body flavor violating mode dominates over the three-body decay $\tilde{t} \to b\,W\,\mathrm{LSP}$.

If the gravitino is the LSP then the decay width for two open decay modes are [35]:

$$\Gamma(\tilde{t} \to bWG) \sim \cos^2 \theta \frac{\alpha}{\sin^2 \theta_W} \frac{(m_{\tilde{t}} - m_W)^7}{128\pi^2 m_W^2 F^2}, \tag{3.5}$$

$$\Gamma(\tilde{t} \to jG) \sim \sin^2 \theta \frac{m_{\tilde{t}}^5}{16\pi F^2}, \tag{3.6}$$

where $\sqrt{F}$ is the SUSY breaking scale. The branching ratio for the flavor violating (FV)
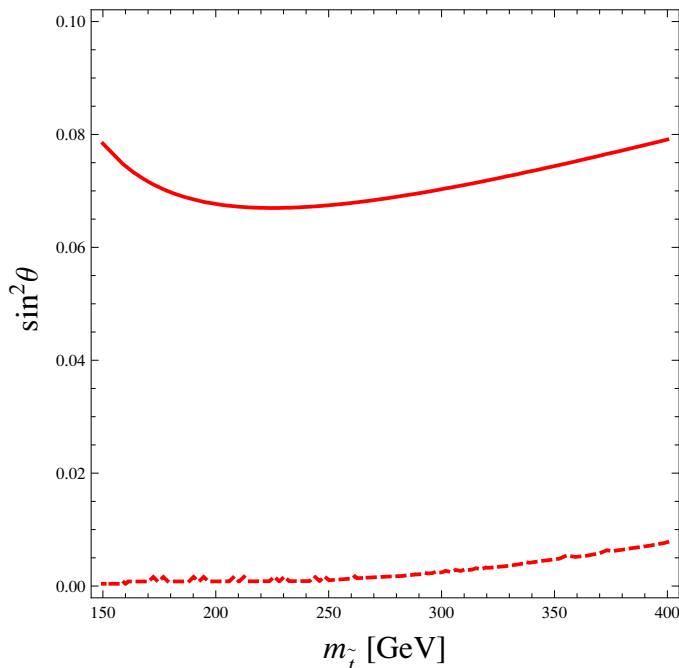
Figure 3. Contour plot for 90% branching ratio for the two-body decay $\tilde{t}_L \to jLSP$ for a bino LSP (solid) and a gravitino LSP (dashed), for $m_{\tilde{t}} - m_{LSP} = 150\,\text{GeV}$. A similar plot applies to the $\tilde{t}_R$ decay modes.

two-body decay is:

$$Br(\tilde{t} \to jG) = \cfrac{1}{1 + \cot\theta^2 \left(\cfrac{\alpha m_{\tilde{t}}^2 (1 - \frac{m_w}{m_{\tilde{t}}})^7}{8\pi \sin^2\theta_W m_W^2} \right)} \tag{3.7}$$

When the gravitino is the LSP the two-body decay mode dominates over three-body decays even for very small mixing angles, as shown in figure 3. This decay mode is prompt for a low SUSY breaking scale ($\sqrt{F} \lesssim 100\,\text{TeV}$). For these SUSY breaking scales the gravitino is extremely light and hence in the following we will take it to be massless. If the LSP is purely bino, the two-body decay dominates (with branching ratio greater than 90%) over the three-body decay for a larger mixing angle (around $\sin^2\theta \sim 0.08$) than in the gravitino case as it shown in figure 3 for a left handed stop (the same conclusion applies to $\tilde{t}_R$). We conclude then that the FV two-body decay mode is the dominant decay mode for the stop in the entire region of the parameter space where $m_{\tilde{t}} < m_t + m_{LSP}$ for moderate mixing. Also, as shown above, the region where it dominates extends above the $m_{\tilde{t}} = m_t + m_{LSP}$ threshold into the so-called stealth region. Therefore, the decay mode into jet plus LSP is a potential discovery mode for a stop NLSP almost degenerate with the LSP. It is interesting to briefly compare the FV stop decay mode in our scenario with the MSSM with minimal flavor violation (MFV). In the MSSM the dominant decay mode is the 3-body decay into bW plus the LSP, and when this is kinematically closed ($m_{\tilde{t}} - m_{LSP} < m_W + m_b$) the dominant decay mode is either the loop suppressed two-body flavor violating (FV) decay mode, $\tilde{t} \to c+\text{LSP}$ or the four body decay. The FV stop decay mode is suppressed compared to the three-body decay since the effective coupling $\tilde{t}\,\chi_0^1\,c$ is of order 10^{-5} assuming MFV (see [36–38]).

4 LHC sensitivity to a light stop NLSP with large flavor mixing

In the previous section we showed that the FV decay mode into a light jet (either a charm or up-quark initiated) and the LSP is the dominant decay mode and hence a potential discovery mode for a stop almost degenerate with the LSP when a moderate squark flavor mixing is present. It is therefore interesting to determine the LHC sensitivity for this topology, and the bounds on the stop mass in this region of the parameter space.

The Tevatron already puts interesting constraints on stops decaying into charm jets. Both D0 [39] and CDF [40] have performed a dedicated analysis for $\tilde{t} \to c$+LSP, putting a bound on the stop mass as strong as $180\,\mathrm{GeV}$ for a $90\,\mathrm{GeV}$ LSP. However, both the more compressed region $\Delta M < 40\,\mathrm{GeV}$ and the region outside $m_{\tilde{t}} - m_{\tilde{B}} < m_W + m_b$, were left unconstrained. These analyses rely on c-tagging, and hence do not directly constrain the FV stop decay into an up quark.

ATLAS and CMS do not have any dedicated analysis for this topology — light stops are searched in the $\tilde{\chi}_1^\pm b$ channel [41]. Nonetheless, since our final state contains missing energy and two jets, jets plus missing energy (MET) LHC searches are potentially sensitive to this topology. Limits on our case can be derived from simplified models for squark searches with decoupled gluinos. However, CMS and ATLAS analyses do not extend to the region of the parameter space significant for us, that is $m_{\tilde{t}} < 300\,\mathrm{GeV}$ and/or $\Delta M = m_{\tilde{t}} - m_{LSP} < m_t$. The reason is that signal efficiency relies in part on the presence of initial state radiation which is associated with large uncertainty. Therefore, our model is largely unconstrained by the LHC analyses, allowing for a stop as light as $100\,\mathrm{GeV}$, the bound from LEP [42]. Dedicated searches for $\tilde{b}_L \to b$+LSP can potentially constrain the left-handed stop significantly. In this paper we will focus on the LHC sensitivity to the flavor mixed stop signals only.

Beyond this particular topology, in general there is an insufficient coverage of the phenomenology of a light stop somewhat degenerate with the LSP in a large region of the available parameter space. Motivated by this lack of coverage several external analyses [43–48] have shown that LHC is sensitive to a broader region of the parameter space than the one explored by the public analyses. [43] and [44] analyze the LHC sensitivity for the stop four body decay, and a bound on its mass of around $250\,\mathrm{GeV}$ was estimated. Furthermore, [43] discuss the FV stop decay, focusing on the region $m_{\tilde{t}} - m_{\tilde{B}} < m_W + m_b$ where the FV mode could dominate even in the MSSM. In [45] a model independent study was performed, and the FV stop decay into a light jet plus the LSP was investigated beyond this particular compressed region. A bound of $\sim 300\,\mathrm{GeV}$ on the stop mass was derived from shape-based hadronic analyses and monojet searches [49, 50].

In this section we will study a simplified model where the stop decays with a 100% branching ratio to j+LSP. We simulate the stop production in MadGraph5 [51]. The stops are then decayed and the decay products hadronized in Pythia [52], which also adds initial and final state showers. Since we are interested in hard jets arising from this radiation, we simulate $\tilde{t}^*\tilde{t}$, $\tilde{t}^*\tilde{t} + j$ and $\tilde{t}^*\tilde{t} + 2j$ at the matrix element level and match it with the Pythia shower. We use a MLM matching scheme with p_T-ordered showers with a QCUT=$100\,\mathrm{GeV}$, which is suitable for heavy pair-production. We use PGS [53] to simulate detector effects

on our signal. The detector simulation and the QCD modeling are probably the strongest limiting factors of our simulation. We emulate relevant LHC analyses for our topology.

4.1 Jets+MET searches

Traditional jets+MET searches both of ATLAS and CMS are designed for QCD production for new physics particles such as squarks or gluinos, which subsequently decay into jets and the LSP — which escapes detection — leading to a missing energy signature.

For spectra with a mass large splitting with the LSP, these searches are very effective. The limits on squark simplified models are crossing the TeV threshold. However, these limits are considerably weakened if only one quark eigenstate is light [54], even if the LSP is massless. The sensitivity of these searches is much worse for the compressed region (for instance, for our region of interest, $m_{\tilde{q}} - m_{LSP} \lesssim m_t$). Most of the data for these searches comes from high instantaneous luminosity samples. Consequently, the hadronic triggers relevant for these searches require a very high amount of hadronic activity ($H_T + E_T \gtrsim$ 1200 GeV for relevant signal regions in the 4.7 fb^{-1} ATLAS analysis, and $H_T > 500$ GeV for the 4.98 fb^{-1} CMS sample [55]). Therefore, these searches are very insensitive to our region of interest. The dedicated searches for the sbottom decaying into b+LSP [56] could be potentially sensitive to our topology since a charm has a 10% probability to be mistagged as a b-quark. It would be then be interesting to recast the dedicated searches for third generation squarks as done in [43] , but extending the region of the parameter space. The possibility of a large squark mixing with a c-quark final state could provide a motivation for an improved c-tagging.

4.2 Shape-based searches

Shape-based analyses like the CMS α_T and the CMS razor analyses [57–59] are much more sensitive to our topology. Instead of only using the overall energy scale in the event, these searches also employ an event shape-based discriminant. This allows the use of shape-based triggers requiring much lower H_T thresholds. We derive limits in the stop-LSP mass plane for a large region of parameter space. We scan over the entire plane (beyond the compressed region) assuming a 100% branching ratio to jet + LSP. While this might be an oversimplification for a realistic model (for example, the single top channel, if open, might provide stronger limits), it allows us to investigate the efficiency of this particular topology in a model independent way. We provide details on the validation of our analysis with published CMS analyses in appendix A.

4.2.1 α_T analysis

The CMS SUSY hadronic searches employing α_T [60] are sensitive to events with 2 or more energetic jets with missing energy. The α_T variable was first discussed in [61]. Since the additional trigger on α_T allows the H_T and p_T thresholds to be significantly lowered, these searches are more sensitive to our region over traditional jets+MET searches.

In this type of analysis all events are clustered into a dijet topology containing two pseudo-jets, choosing the combination which minimizes the E_T difference between the two pseudo-jets.
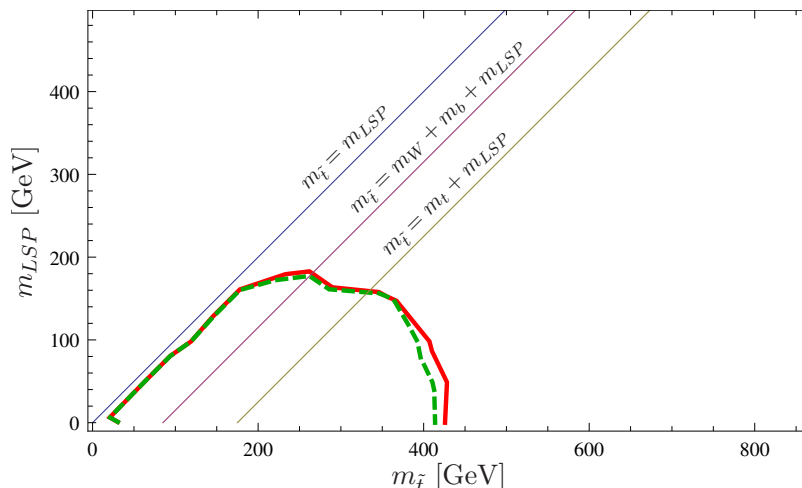
Figure 4. Limits from the 7 TeV α_T analysis in the $(m_{\tilde{t}}, m_{LSP})$ plane. The solid red line indicates the observed limit, while the dashed green line shows the expected limit. The stop is assumed to decay into jet and LSP with 100% branching ratio everywhere.

The variable α_T is defined as,

$$\alpha_T = \frac{E_T^{j_2}}{M_T} \qquad M_T = \sqrt{(E_T^{j_1} + E_T^{j_2})^2 - (p_x^{j_1} + p_x^{j_2})^2 - (p_y^{j_1} + p_y^{j_2})^2} \qquad (4.1)$$

where E_T for each pseudo-jet is defined as the scalar sum of p_T of its components.

Jets considered in the analysis are required to have $E_T > 50\,\text{GeV}$. Further, the two highest-E_T jets must satisfy $E_T > 100\,\text{GeV}$ each, and the highest E_T jet should be central, $|\eta| < 2.5$. Events with additional hard jets ($E_T > 50\,\text{GeV}$) are vetoed if the jet $|\eta| > 3.0$. Events are also required to have significant hadronic activity $H_T > 275\,\text{GeV}$. Finally, a requirement of $\alpha_T > 0.55$ brings the QCD backgrounds down to manageable levels. Events which pass these requirements are categorised according to their H_T. The p_T thresholds in the lowest two H_T bins are rescaled to keep the efficiency of the α_T cut similar in each H_T region.

The CMS analysis [60] does not cover the parameter space we are interested in. We emulate the α_T analysis on our simulated sample (the limits are presented in figure 4 and figure 5). The experimental limit is calculated using a likelihood model to test for the presence of a variety of signal models. We employ the frequentist-Bayesian hybrid variant of the CLs method [62, 63] to put 95% limits on our signal. The CLs method is known to give conservative statistical limits, especially when the data under-fluctuates with respect to the background expectation (as is the case for this analysis).

Our 95% level CLs limits, computed for a single stop eigenstate decaying a 100% into jet and the LSP, are presented in the stop-LSP mass plane in figure 4. Our estimate excludes a single stop $\tilde{t}$ below 250 GeV in the highly compressed region $\Delta M < m_W + m_b + m_{LSP}$, while for an increased mass splitting ($\Delta M \sim 150\,\text{GeV}$) the limit is around 350 GeV. Stop masses below $\sim 420\,\text{GeV}$ are excluded for massless LSP. The interpretation of the actual limit within a realistic model with mixing is not straightforward since for $\Delta M > m_t$ the
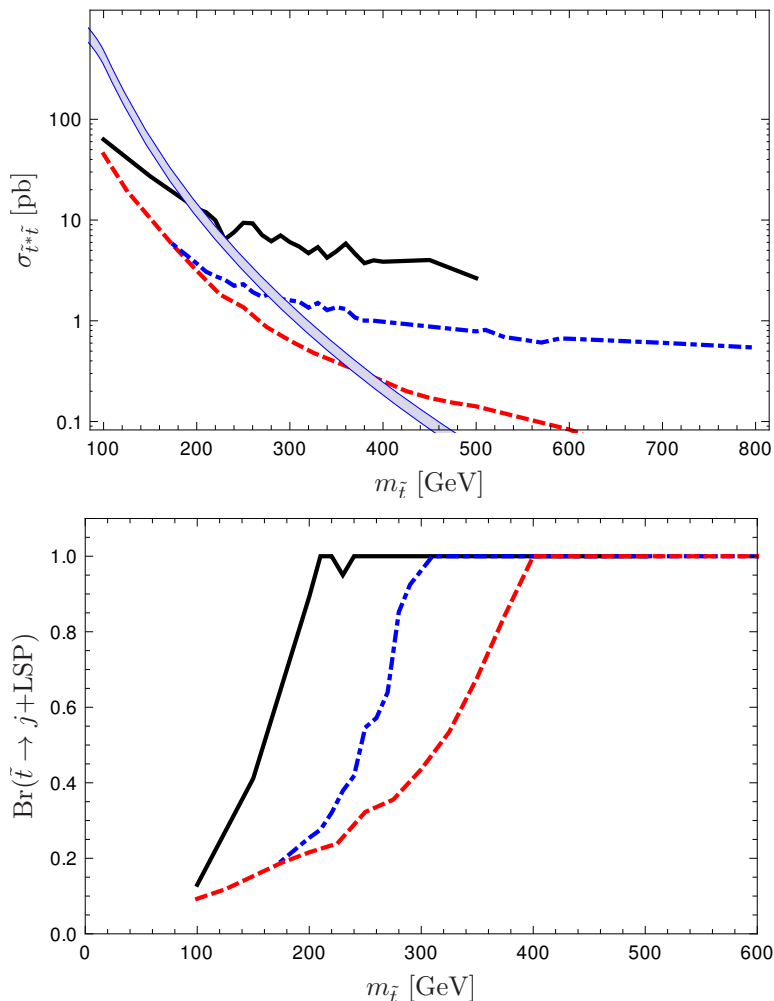
Figure 5. Cross section (top) and branching ratio (bottom) limits from the 7 TeV α_T analysis as a function of stop mass for various LSP masses, (solid black $m_{\tilde{t}} - m_{\tilde{B}} = 10\,\text{GeV}$, dot-dashed blue: $m_{\tilde{t}} - m_{\tilde{B}} = 150\,\text{GeV}$, dashed red: $m_{\tilde{B}} = 0\,\text{GeV}$ and $m_{3/2} = 0\,\text{GeV}$). The gray band is the NLO stop production cross section at 7 TeV computed using Prospino 2.1 [64].

decay mode into j+LSP is no longer the dominant decay mode, and therefore the branching ratio suppression has to be taken into account.

The left plot in figure 5 shows the 95% limit on the cross section for different mass splittings, $200\,\text{GeV} < \Delta M < 250\,\text{GeV}$. Also, we interpret these as limit on the branching ratio as a function of the stop mass. We notice that the cross section limits are relatively flat in $m_{\tilde{t}}$, while the stop production cross section is steeply falling. Thus, the branching ratio suppression does not result in a significantly different limit. At the same time, when we add additional states at the same mass (for instance, $\tilde{t}_R, \tilde{t}_L$ and $\tilde{b}_L$ all together or just $\tilde{t}_L$ and $\tilde{b}_L$) the cross section gets multiplied by a factor of 2 or 3. By the same logic, these limits do not get much worse in this case.

The plot in figure 6 shows the limits on the stop mass in the region $\Delta M > m_t$ for a massless LSP for different values of the mixing angle. For a gravitino LSP, for mixing
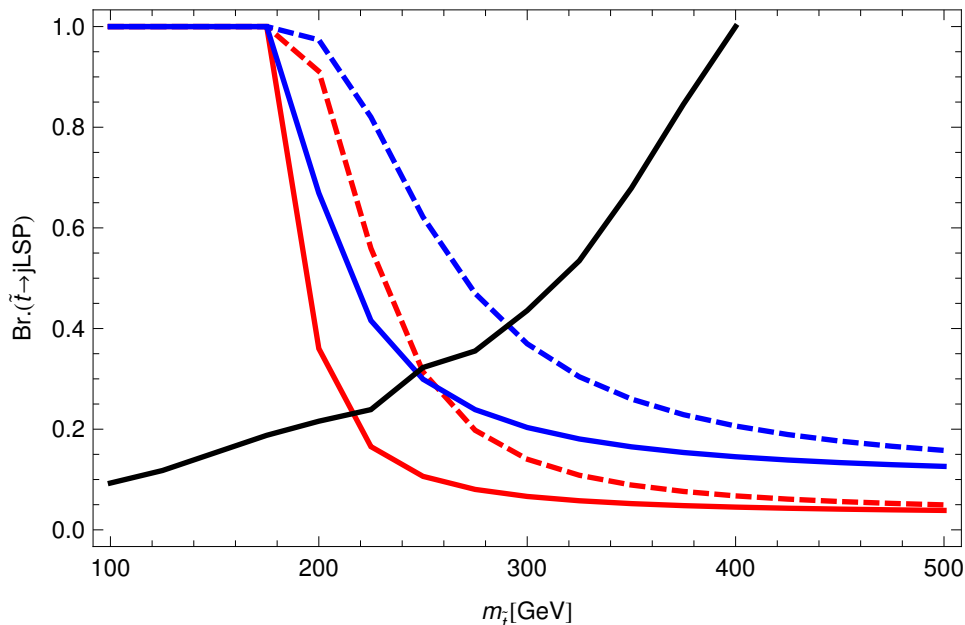
Figure 6. The limit on the branching ratio $\tilde{t} \to jLSP$ as a function of the stop mass (black solid). The different curves represent branching ratios for $\tilde{t} \to j\tilde{G}$ (dashed) and $\tilde{t} \to j\tilde{B}$ (solid) considering $\sin^2 \theta = 0.03$ (red) and 0.1(blue). The LSP is always assumed to be massless.

as low as 3% the entire stealth region $m_{\tilde{t}} \lesssim 250 \, \text{GeV}$ is excluded. For a massless bino instead, the stealth region is ruled out for a larger mixing angle $\sin^2 \theta \sim 0.1$. For a heavier stop, dedicated searches for t+LSP decay mode start to be sensitive setting a limit which depends on the amount of mixing. Stops of mass up to $500 \, \text{GeV}$ are excluded even in the maximal mixed scenario [34]. Therefore, the natural window for a massless LSP and a mixed stop could be almost entirely covered.

4.2.2 Razor analysis

The razor is an inclusive analysis which divides the signal and background into various boxes based on the final states. A global limit can then be derived from a likelihood analysis over every box. The power of the analysis lies in the fact that the backgrounds in each of the boxes are well-fit by a simple function, hence allowing for a relatively small error in the background extrapolation into the signal region. In our case, the signal only populates the HadBox (defined below), and hence all limits will be derived from this box only.

The razor search is designed to look for pair production of new heavy states which yield high energy jets. All events are clustered into two megajets to reduce every final state into the dijet topology. The two razor variables employed, M_R and R are then calculated from these megajets. The M_R razor kinematic variable is given as,

$$M_R = \left[(|\vec{p}^{j_1}| + |\vec{p}^{j_2}|)^2 - (p_z^{j_1} + p_z^{j_2})^2 \right]^{\frac{1}{2}} \tag{4.2}$$

and is invariant under longitudinal boosts. M_R approximates the energy scale in the heavy

particle decay and peaks at,

$$M_\Delta = \frac{m_{\tilde{t}}^2 - m_{LSP}^2}{m_{\tilde{t}}} \qquad (4.3)$$

The R variable is defined as

$$R = M_T^R/M_R, \qquad (4.4)$$

where $M_T^R \leq M_\Delta$ is a transverse invariant mass, defined as,

$$M_T^R = \left[\frac{1}{2} \left(E_T^{miss}(p_T^{j_1} + p_T^{j_2}) - \vec{E}_T^{miss} \cdot (\vec{p}_T^{j_1} + \vec{p}_T^{j_2}) \right) \right]^{\frac{1}{2}} \qquad (4.5)$$

QCD jets typically have a small value of R, and the QCD distribution peaks at $R \sim 0$, whereas the heavy particle production can produce higher values of R.

In the compressed region, much of the jet activity arises from QCD radiation, and hence the above observations are not directly applicable. The M_R and R^2 distributions depend weakly on the stop mass, but are largely determined by the jet p_T selection. Therefore, it is remarkable that the razor searches are effective in this region of parameter space. In fact, we find that the razor analysis limits go all the way to the degeneracy limit ($m_{\tilde{t}} = m_{LSP}$), where the stop decay products are not visible, and all hadronic activity arises purely from initial and final state radiation. It has been pointed out that in this region, the stop search is analogous to the dark matter search ([44, 65]). For the same reason, the monojet analysis designed for dark matter search sets significant limits on the stop masses for a very compressed spectrum ($\Delta M < 30 - 40\,\text{GeV}$) [43–46].

As mentioned above, the only box relevant for our simplified model is the HadBox. An event is put into the HadBox if it does not fall into any other Box (involving electron and/or muon final states), and satisfies $M_R > 400\,\text{GeV}$ and $0.18 < R^2 < 0.5$, [57].

The crucial feature of this search driving the limits in our case is the relatively low p_T thresholds. All jets with $p_T > 40\,\text{GeV}$ and $|\eta| < 3.0$ are considered. There is a further requirement on the two highest-p_T jets to have $p_T > 60\,\text{GeV}$.

The limits are derived according to the procedure outlined in [44]. From each box (which in our case is just one box), a posterior-probability density function is derived for the signal cross section,

$$P(\sigma) = \int_0^\infty db \int_0^1 d\epsilon \frac{(b + L\sigma\epsilon)^n e^{-b-L\sigma\epsilon}}{n!} \text{lognormal}(\epsilon|\bar{\epsilon}, \delta_\epsilon) \text{lognormal}(b|\bar{b}, \delta_b) \qquad (4.6)$$

where b is the actual background yield, $\bar{b}$ is the expected background yield and δ_b is the error in the background modeled using a lognormal distribution. The corresponding quantities for ϵ denote the efficiencies. An error of 30% was chosen for the signal efficiency to account for detector simulation errors. σ is the cross section, n the observed number of events and L is the available luminosity. The 95% limit is then straightforwardly derived from the cumulative distribution of $P(\sigma)$. In figure 7 and figure 8 we show the limits obtained. Our results are consistent with results in the literature [44, 45] to the extent they can be compared.
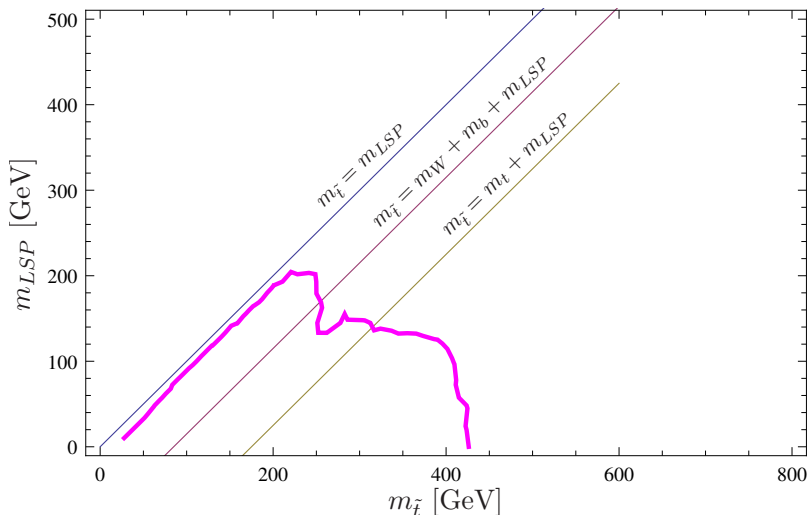
Figure 7. Limits on our scenario from the 7 TeV razor analysis [57] in the $(m_{\tilde{t}}, m_{LSP})$ plane. The stop is assumed to decay into jet and LSP with 100% branching ratio everywhere.

We present the limits in the stop-LSP mass plane in figure 7, and the limits on the cross section and the branching ratio in figure 8. Similar conclusions as the α_T search hold. The limit is insensitive to the stop mass, and hence branching ratio suppression or multiplicity enhancements do not change the limits significantly.

Extending the razor

The razor analysis appears to be applicable beyond its design topology. This was already noted in previous analyses [44, 65]. In particular, it is one of the strongest bounds on the signatures considered in this paper. We comment briefly on the possibility of extending the current analysis strategy to improve the sensitivity to our signal.

In figure 9 we plot the two-dimensional histogram of the number of events expected at the LHC at 5 fb^{-1} as a function of the razor variables, m_R and R^2 for two mass spectra as examples. We see that for $m_{\tilde{t}} = 500\,\text{GeV}$, $m_{\tilde{B}} = 0\,\text{GeV}$, the events populate high m_R bins, and hence would tend to pass the analysis cuts. For $m_{\tilde{t}} = 500\,\text{GeV}$, $m_{\tilde{B}} = 340\,\text{GeV}$, the m_R spectrum is significantly softer. However, the events are pushed towards larger R^2 values, where the QCD background is expected to be minimal. Therefore, extending the razor signal region to include the low m_R - high R^2 region could potentially improve the sensitivity to the signal.

5 Conclusions

We have explored a scenario where the third generation squarks mix significantly with either the first or the second generation. This arises generically (both in the left and the right-handed sector) in models with an approximate R-symmetry, but at the same time, these results also apply to MSSM scenarios beyond MFV where the right handed stop mixes with the charm (for instance in the scenario described in [34]). These frameworks are especially interesting in light of the recent LHC null results for degenerate squarks.
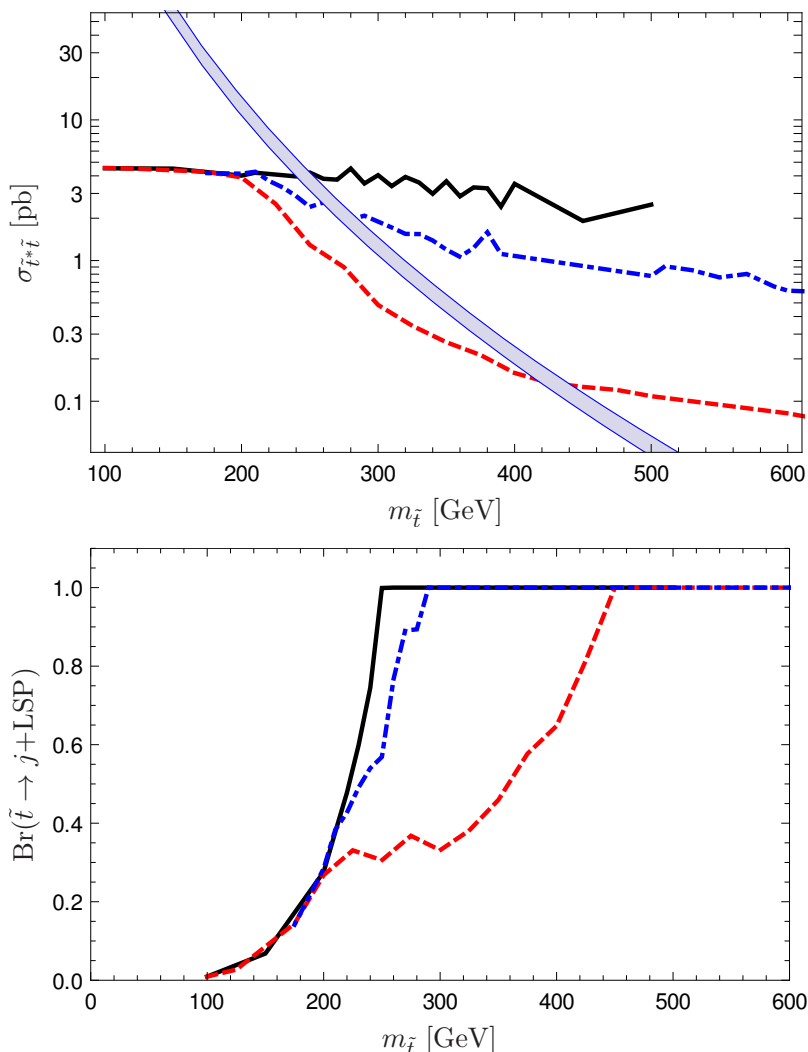
Figure 8. Cross section (top) and branching ratio (bottom) limits from the 7 TeV razor analysis as a function of stop mass for various LSP masses, (solid black $m_{\tilde{t}} - m_{\tilde{B}} = 10 \, \text{GeV}$, dot-dashed blue: $m_{\tilde{t}} - m_{\tilde{B}} = 150 \, \text{GeV}$, dashed red: $m_{\tilde{B}} = 0 \, \text{GeV}$ and $m_{3/2} = 0 \, \text{GeV}$). The gray band is the NLO stop production cross section at 7 TeV computed using Prospino 2.1 [64].

Also, independent of theoretical arguments, it is important to make sure that the LHC has a good coverage of SUSY scenarios beyond MSSM.

In this paper we have focused in particular on a light stop somewhat degenerate with the LSP. We study the FV decay topology, $\tilde{t} \rightarrow j$ LSP, which dominates in an extended region of the parameter space for moderately large mixing. This region is unconstrained in the public analyses of ATLAS and CMS. However, our emulation of the CMS razor and α_T searches [57, 66] seem to be sensitive to this region of the parameter space and are able to rule out a significant portion of it. This is in agreement with recent work on light stop phenomenology, [43–46]. For a massive bino we find that the bounds on the stop mass varies between 250 GeV and 350 GeV depending on the mass splitting between the stop and the bino. For a massless bino the bound on FV decay mode rules out all the stealth
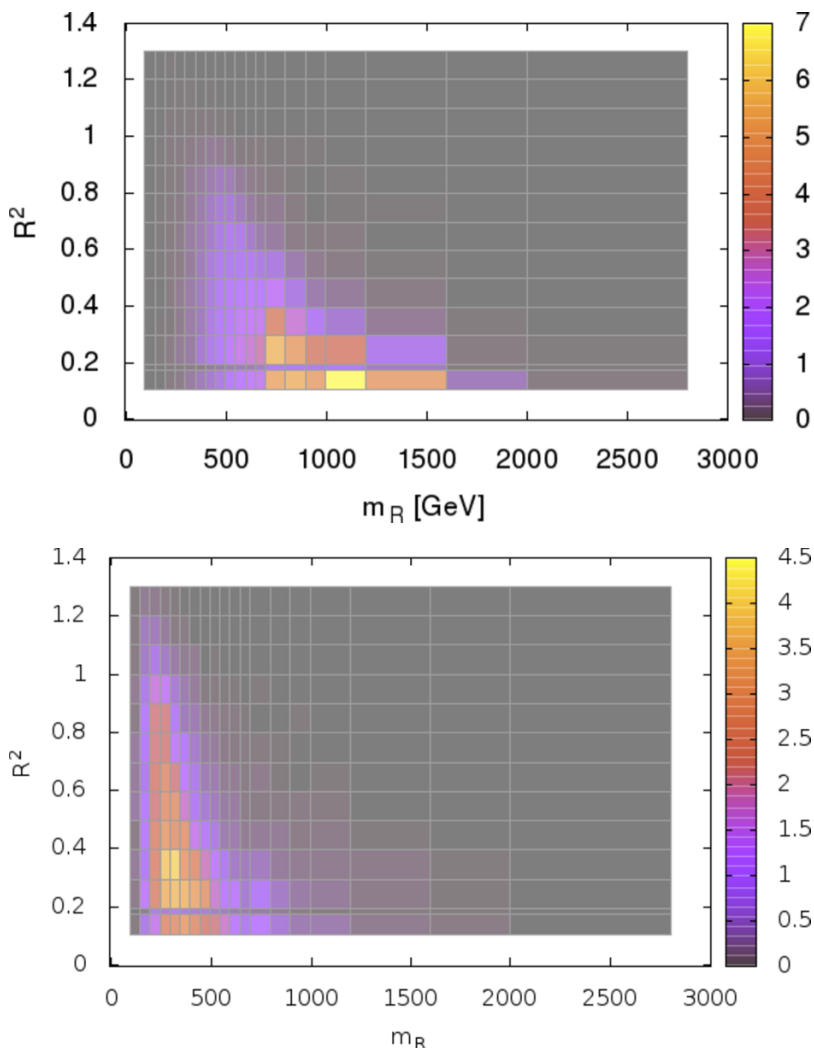
Figure 9. Two-dimensional histograms for the number of events at 4.7 fb^{-1} in m_R and R^2 plane for $m_{\tilde{t}} = 500\,\text{GeV}$, $m_{\tilde{B}} = 0\,\text{GeV}$ (top) and $m_{\tilde{t}} = 500\,\text{GeV}$, $m_{\tilde{B}} = 340\,\text{GeV}$ (bottom).

region ($m_{\tilde{t}} < 250\,\text{GeV}$) as long as mixing is around 10%. For a massless gravitino LSP, a stop below 250 GeV is ruled by the FV decay mode for an even smaller mixing, 3%. For heavier masses the dedicated searches for $\tilde{t} \to t$ LSP start to be efficient, setting a bound in the 500-560 GeV range (depending on the mixing).

These light stop bounds involve extending searches in regions beyond where they were designed to operate. There is a potential danger that this might not always be possible. For instance, the CMS razor analysis [67] attempting to put limits in the mass region $m_{\tilde{q}} < 300\,\text{GeV}$ and $m_{\tilde{q}} - m_{LSP} < 150\,\text{GeV}$ finds that this region has a sensitivity to the ISR modeling in simulation of signal events above a pre-defined tolerance; hence no interpretation is presented for these model points. We expect that improved analyses can probe this region effectively.

It is important to extend the LHC searches for light stops to all possible channels unrestricted by theoretical bias. As an example we show that a light stop can have sig-

natures similar to a first or second generation squark in a significant region of parameter space. This is especially relevant for the 7-8 TeV run of the LHC, since at 13 TeV, the QCD backgrounds for jets+MET searches get even worse relative to the background for third generation final states. This could make our topology challenging to look for and potentially a blind spot for light stops.

Acknowledgments

A   Validation of analyses

In this appendix, we compare our emulation of the α_T analysis with published results in the context of the "squark simplified model", considering the direct production of squarks with the gluinos decoupled. The signature is jets with missing energy, identical to the signal considered in this paper for the flavor violating stop decays.

In figure 10 we compare the 95% CLs limits extracted from the experiment. Both the observed and the expected limits are shown. We also show 95% CLs bounds on our signal following the same procedure as the experimental search. The background systematic uncertainties are modeled using an asymmetric log-normal distribution, and are based on the numbers in the LHC search. We do not include a systematic error on the signal. Varying the signal systematic error up to 30% was seen to only mildly weaken the limits. The limits were obtained by using the LandS tool using the frequentist-Bayesian Hybrid style CLs with log-normal background systematic errors.

We find that our limits are in agreement within the 1σ theoretical and experimental error bands with the CMS limits in the uncompressed region . This is the region in which our limits can be directly compared with the experimental analysis. Close to the degeneracy line, $(m_{\tilde{t}} \sim m_\chi)$, the experimental analysis does not report a limit due to unreliability of initial state radiation modeling. While matrix element level simulation is performed for the background estimation, the analysis used only Pythia to simulate their signal, which uses showering of the initial state and final state partons to produce additional jets. In the region of phase space where this radiation has high p_T, the showering approximation breaks down, leading to unreliable results. Our simulation for the signal was done at the matrix element level for up to two hard jets, matched with Pythia using the p_T-ordered MLM scheme at QCUT=100 GeV. The presence of a hard ISR jet is crucial to pass the selection cuts in the compressed region, so the systematic errors introduced in the matching procedure can potentially weaken the limits. In order to show the robustness of the limits in this region, in figure 10 we also plot regions of parameter space which are ruled out by a factor of 2. While this is obviously a smaller region of parameter space, there is no significant
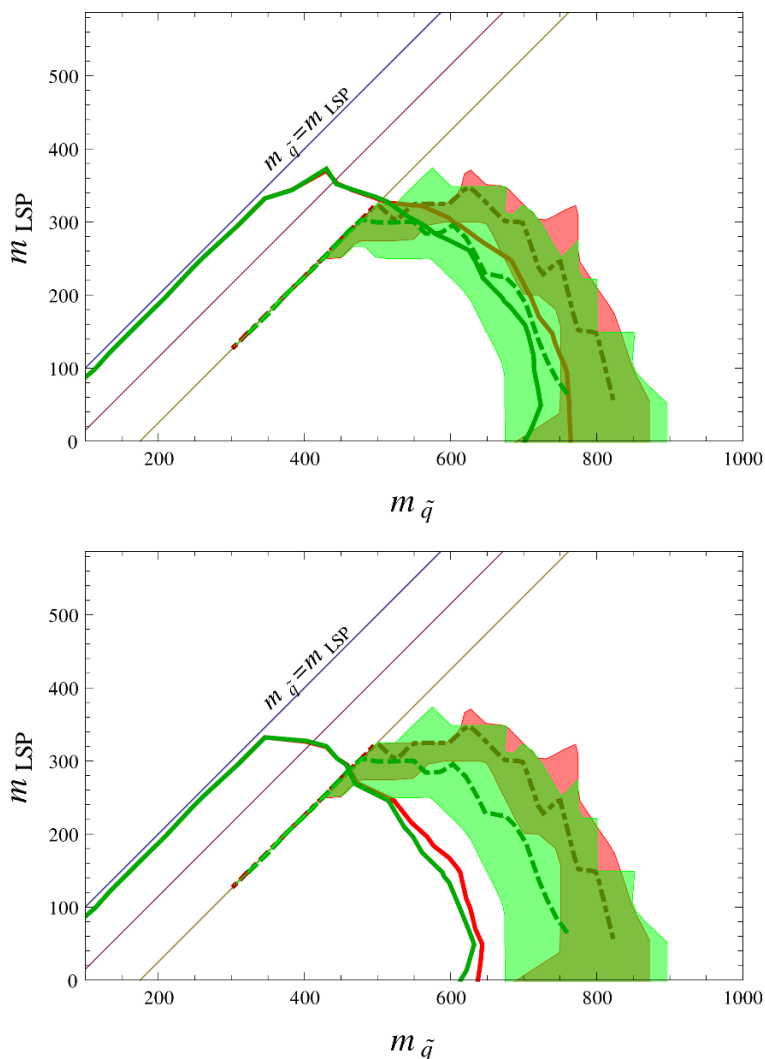
Figure 10. Comparison of limits from the CMS α_T analysis [60] with our analysis in the simplified squark model as a function of the masses $(m_{\tilde{q}}, m_{LSP})$. The red dot-dashed line indicates the observed limit, along with $\pm 1\sigma$ shaded band obtained by varying the theory prediction by its NLO error. The dashed green line shows the expected limit, along with $\pm 1\sigma$ shaded band for the expected limit. The observed (red solid) and expected (green solid) limits obtained from our analysis are also shown. The lower plot shows the parameter space which is excluded by more than a factor of 2 in our analysis.

degradation of the limit near the degeneracy line. Therefore, the presence of hard ISR does not invalidate our limits, and we show that the limits in fact extend through to the degeneracy line. Our simulations stop at $m_{\tilde{t}} - m_{\chi} = 10\,\mathrm{GeV}$. Beyond this point, the narrow width approximation is not always applicable and a more careful analysis incorporating the width of the stop needs to be performed. However, it seems unlikely that this would qualitatively change the nature of the limits. We leave this possibility for future work.

We are unable to perform a similar exercise for the razor search, since the particular search we use only provides an interpretation in terms of the CMSSM, and not in terms of

a simplified squark model. Even for that model, the analysis uses an unbinned extended likelihood method, whereas the only data and background estimates provided are binned coarsely into 6 signal regions. Therefore, even under ideal circumstances it would be difficult to reproduce their efficiencies.

Fortunately, a detailed description of a method for adapting the razor analysis to generic SUSY searches was made available publicly [68], which we use extensively. This emulation was compared with published experimental limits and was found to be in reasonable agreement, if slightly conservative. Similar methodology was adopted in a number of theoretical emulations of the razor analysis [44, 46]. This procedure allocates a generous 30% error for the modeling of the detector efficiency, leading to conservative estimates of the bound. The bound obtained was seen to have only a mild dependence on this error estimate.

B Flavor constraints in R-symmetric models

In this appendix we will briefly review how a quasi-exact R-symmetry alleviates the flavor problem of low energy supersymmetry (see [11] for a detailed discussion). For this purpose let us define the mixing parameters δ_{ij}^L and δ_{ij}^R, namely:

$$\delta_{ij}^{L/R} = \frac{m_{ij}^2}{M_{\tilde{q}}^2}, \tag{B.1}$$

where m_{ij}^2 are the off diagonal elements of the squark mass matrix and $M_{\tilde{q}}^2$ is the average of the diagonal mass entries.

The mixing in the first and second generation is mostly constrained by the observations in the $K^0 - \bar{K}^0$ system. In the MSSM the effective Hamiltonian for $K^0 - \bar{K}^0$ mixing gets contributions, among others, from the diagrams like figure 11. This leads to strong constraints on the amount of mixing, for instance the measurement of ΔM leads to severely constraints on $\text{Re}[\delta_{ii}]$, $\text{Re}[\delta_{ii}] < 0.003$, with $i = L, R$ and $m_{\tilde{q}} \sim 800\,\text{GeV}$ and $m_{\tilde{g}} \sim 1.5\,\text{TeV}$.

In R-symmetric models the constraints from $K^0 - \bar{K}^0$ mixing are relaxed since the dimension 5 operators:

$$\frac{1}{m_{\tilde{g}}} \tilde{d}_R^* \tilde{s}_L^* \bar{d}_R s_L, \tag{B.2}$$

are forbidden by the R symmetry. $\tilde{d}_R^*$ and $\tilde{s}_L^*$ have the same R charge, while the corresponding fermions are neutral. The leading operators are then dimension 6 operators which decouple faster than the dimension 5 contribution ($\frac{m_{\tilde{q}}^2}{m_{\tilde{g}}^4}$ as opposed to $\frac{1}{m_{\tilde{g}}^2}$). Furthermore, in R-symmetric models the (Dirac) gluinos can be naturally much heavier than the squarks ($m_{\tilde{g}} \sim 10 m_{\tilde{q}}$), therefore the limit $m_{\tilde{g}} \gg m_{\tilde{q}}$ is not fine-tuned. These two features taken together help in suppressing the SUSY contributions to flavor observables, allowing $\mathcal{O}(1)$ flavor violation (in the real part) event for light (subTeV) squarks.[3] However, the

---

[3]It is important to notice that, as it is shown in [13] QCD corrections to this flavor observable turn out to be significant, and taking them into account, the mixing is now restricted to be of order 0.1 for relatively light gluinos and squarks.
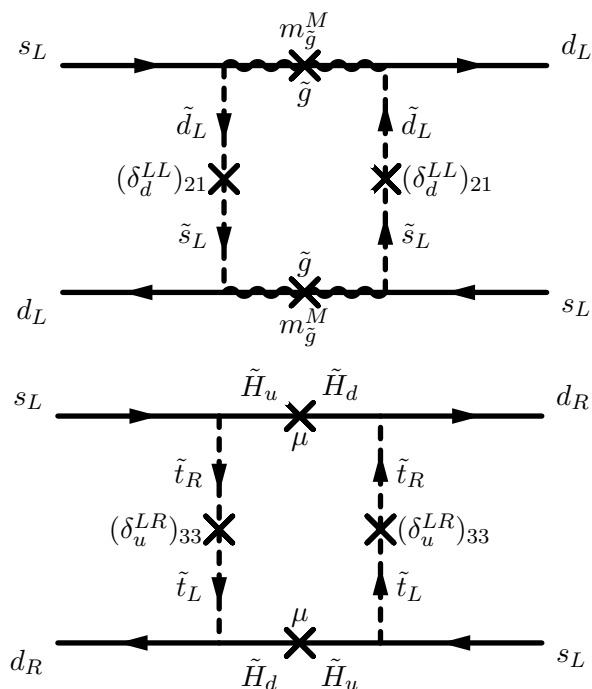
Figure 11. Representative diagrams contributing to $K - \bar{K}$ mixing. The R-symmetry violating terms are explicitly shown as insertions.
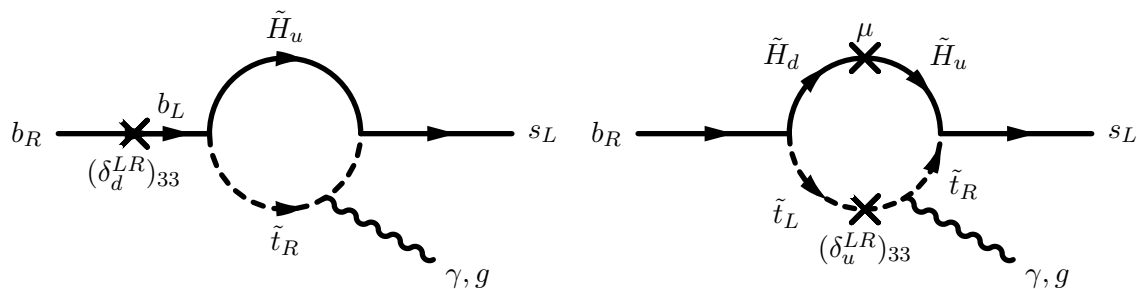

Figure 12. $b \to s\gamma$.

imaginary part of this mixing is severely constrained by the measurement of ϵ_K. Therefore, the mixing in the first and second generation still requires mild flavor structure in order to be consistent with the limits. For B meson mixing the suppression of the box diagrams discussed in the context of $K - \bar{K}$ mixing continue to apply, with the appropriate replacement. This observable does not lead to significant constraints on the $d\,b$ sector from B meson mixing. Similar R-symmetry violating insertions are needed for $\Delta F = 1$ flavor observables, such as $b \to s\gamma$, and constraints are significantly weakened in the presence of the R-symmetry.

The dominant contribution to this process within the MSSM involves coupling of opposite helicity states which arise from a helicity flip on the gaugino line, figure 12. In our scenario the constraints are relaxed by the presence of the R symmetry since it forbids a helicity flip via a Majorana gluino insertion. The only possibility is then to have a helicity
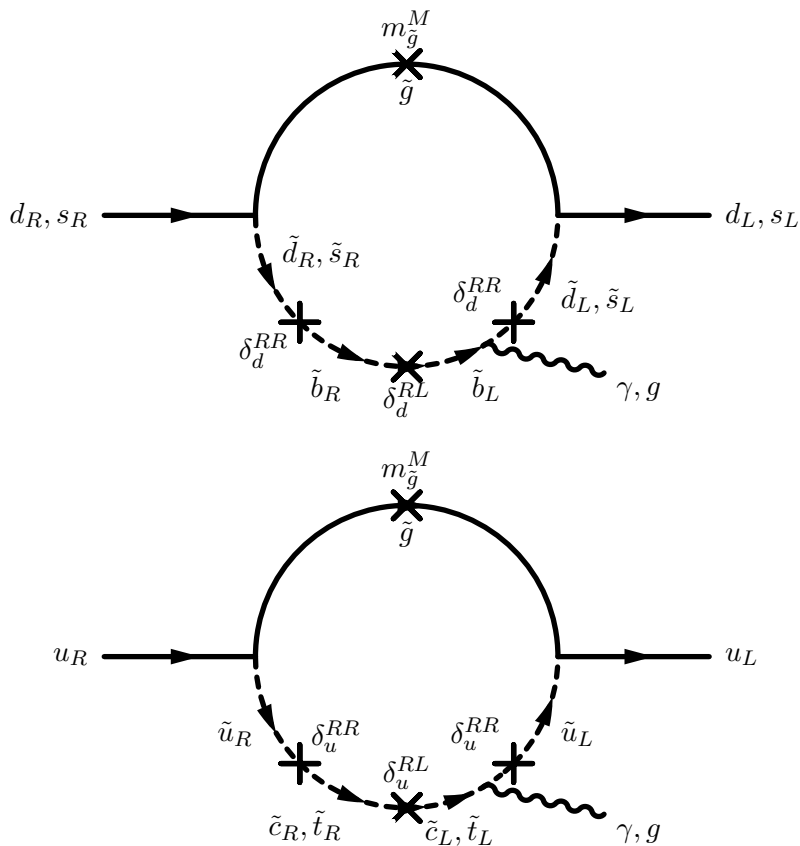
Figure 13. EDM contributions.

flip on the external leg which is more suppressed. Furthermore, the absence of gaugino Majorana mass and μ terms forbids the $\tan \beta$ enhancement of process like $B \to \mu\mu$. Therefore, the mixing of the third generation with the first and the second can be of order one both left and in the right handed sector, see [11]. This is an important different with the MSSM where the bounds on $B_s^0 - \bar{B}_s^0$ mixing and $b \to s\gamma$ significantly constrains the mixing between the third and second generation squarks in the left handed sector. Furthermore, it is important to notice that dangerous contributions to flavor observables can arise from beyond the squark mass mixing. For instance a light stop, which is our case of interest, can give a potentially sizeable contribution to the branching ratio $BR(B \to X_s\gamma)$ or $Br(B \to \mu\mu)$. However, the R symmetry suppresses these contributions. The contribution of a light stop to those processes could arise just through diagram with an external chirality flip. For sufficiently heavy Wino and gluino, the only contribution would arise from $\tilde{t}_R$, namely for $m_{\tilde{t}}^2 \sim \mu$ [44]:

$$\frac{BR(B \to \gamma X_s)}{BR(B \to \gamma X_s)_{SM}} = 1 + \frac{m_t^2}{36m_{\tilde{t}}^2}, \tag{B.3}$$

which is naturally below the experimental limit.

Finally we should comment an another interesting feature of R symmetric SUSY models — the fact that the EDM constraints are absent. The usual one-loop contributions to EDMs

in the MSSM arise from left-right insertions see figure 13, which are completely absent due to the absence of Majorana mass terms, left-right mixing terms. In the purely R-symmetric limit, the one-loop contributions from Dirac gauginos and two-loop contributions from pure gaugino/Higgsino loops are absent. As noted above, the gravitino mass induces a source of R-symmetry breaking, which can potentially induce measurable EDMs.

In this appendix we have briefly summarised the SUSY flavor problem in the context of R symmetric models. Even though it is significantly alleviated, the R-symmetry does not completely solve the flavor puzzle in SUSY. A mild flavor structure (in particular, a suppressed CP-violating phase) is still needed in order to satisfy the bounds from $K - \bar{K}$ mixing. However, many flavor violating observables are absent, and others significantly suppressed. Importantly, these suppressions are obtained independent of the SUSY breaking/mediation paradigm (beyond the requirement of R-symmetry). Therefore, the set of flavor assumptions for a viable R-symmetric SUSY model is much smaller than in the MSSM. In this work we have studied some possible consequences on this on the LHC phenomenology.

References

[1] ATLAS collaboration, *Observation of a new particle in the search for the standard model Higgs boson with the ATLAS detector at the LHC*, *Phys. Lett.* **B 716** (2012) 1 [arXiv:1207.7214] [INSPIRE].

[2] CMS collaboration, *Observation of a new boson at a mass of* 125 *GeV with the CMS experiment at the LHC*, *Phys. Lett.* **B 716** (2012) 30 [arXiv:1207.7235] [INSPIRE].

[3] S. Dimopoulos and D.W. Sutter, *The supersymmetric flavor problem*, *Nucl. Phys.* **B 452** (1995) 496 [hep-ph/9504415] [INSPIRE].

[4] F. Gabbiani, E. Gabrielli, A. Masiero and L. Silvestrini, *A complete analysis of FCNC and CP constraints in general SUSY extensions of the standard model*, *Nucl. Phys.* **B 477** (1996) 321 [hep-ph/9604387] [INSPIRE].

[5] M. Papucci, J.T. Ruderman and A. Weiler, *Natural SUSY endures*, *JHEP* **09** (2012) 035 [arXiv:1110.6926] [INSPIRE].

[6] C. Brust, A. Katz, S. Lawrence and R. Sundrum, *SUSY, the third generation and the LHC*, *JHEP* **03** (2012) 103 [arXiv:1110.6670] [INSPIRE].

[7] G.F. Giudice, M. Nardecchia and A. Romanino, *Hierarchical soft terms and flavor physics*, *Nucl. Phys.* **B 813** (2009) 156 [arXiv:0812.3610] [INSPIRE].

[8] R. Barbieri, E. Bertuzzo, M. Farina, P. Lodone and D. Zhuridov, *Minimal flavour violation with hierarchical squark masses*, *JHEP* **12** (2010) 070 [*Erratum ibid.* **1102** (2011) 044] [arXiv:1011.0730] [INSPIRE].

[9] R. Barbieri, E. Bertuzzo, M. Farina, P. Lodone and D. Pappadopulo, *A non standard supersymmetric spectrum*, *JHEP* **08** (2010) 024 [arXiv:1004.2256] [INSPIRE].

[10] N. Craig, M. McCullough and J. Thaler, *Flavor mediation delivers natural SUSY*, *JHEP* **06** (2012) 046 [arXiv:1203.1622] [INSPIRE].

[11] G.D. Kribs, E. Poppitz and N. Weiner, *Flavor in supersymmetry with an extended R-symmetry*, *Phys. Rev.* **D 78** (2008) 055010 [arXiv:0712.2039] [INSPIRE].

[12] R. Fok and G.D. Kribs, *$\mu \to e$ in R-symmetric supersymmetry*, *Phys. Rev.* **D 82** (2010) 035010 [arXiv:1004.0556] [INSPIRE].

[13] A.E. Blechman and S.-P. Ng, *QCD corrections to K-$\bar{K}$ mixing in R-symmetric supersymmetric models*, *JHEP* **06** (2008) 043 [arXiv:0803.3811] [INSPIRE].

[14] G.D. Kribs, A. Martin and T.S. Roy, *Squark flavor violation at the LHC*, *JHEP* **06** (2009) 042 [arXiv:0901.4105] [INSPIRE].

[15] C. Frugiuele and T. Gregoire, *Making the sneutrino a Higgs with a $U(1)_R$ lepton number*, *Phys. Rev.* **D 85** (2012) 015016 [arXiv:1107.4634] [INSPIRE].

[16] R. Davies, J. March-Russell and M. McCullough, *A supersymmetric one Higgs doublet model*, *JHEP* **04** (2011) 108 [arXiv:1103.1647] [INSPIRE].

[17] C. Frugiuele, T. Gregoire, P. Kumar and E. Ponton, *'L = R' — $U(1)_R$ as the origin of leptonic 'RPV'*, *JHEP* **03** (2013) 156 [arXiv:1210.0541] [INSPIRE].

[18] F. Riva, C. Biggio and A. Pomarol, *Is the 125 GeV Higgs the superpartner of a neutrino?*, *JHEP* **02** (2013) 081 [arXiv:1211.4526] [INSPIRE].

[19] M. Heikinheimo, M. Kellerstein and V. Sanz, *How many supersymmetries?*, *JHEP* **04** (2012) 043 [arXiv:1111.4322] [INSPIRE].

[20] G.D. Kribs and A. Martin, *Supersoft supersymmetry is super-safe*, *Phys. Rev.* **D 85** (2012) 115014 [arXiv:1203.4821] [INSPIRE].

[21] C. Frugiuele, T. Gregoire, P. Kumar and E. Ponton, *'L = R' — $U(1)_R$ lepton number at the LHC*, *JHEP* **05** (2013) 012 [arXiv:1210.5257] [INSPIRE].

[22] P.J. Fox, A.E. Nelson and N. Weiner, *Dirac gaugino masses and supersoft supersymmetry breaking*, *JHEP* **08** (2002) 035 [hep-ph/0206096] [INSPIRE].

[23] R. Barbieri and G. Giudice, *Upper bounds on supersymmetric particle masses*, *Nucl. Phys.* **B 306** (1988) 63 [INSPIRE].

[24] ATLAS collaboration, *Search for squarks and gluinos with the ATLAS detector using final states with jets and missing transverse momentum and $5.8\,fb^{-1}$ of $\sqrt{s} = 8$ TeV proton-proton collision data*, ATLAS-CONF-2012-109 (2012).

[25] G. Bozzi, B. Fuks, B. Herrmann and M. Klasen, *Squark and gaugino hadroproduction and decays in non-minimal flavour violating supersymmetry*, *Nucl. Phys.* **B 787** (2007) 1 [arXiv:0704.1826] [INSPIRE].

[26] P. Agrawal, C. Frugiuele, and C.-T. Yu, *The better tempered neutralino*, work in progress.

[27] M. Perelstein and B. Shakya, *XENON100 implications for naturalness in the MSSM, NMSSM and lambda-SUSY*, *Phys. Rev.* **D 88** (2013) 075003 [arXiv:1208.0833] [INSPIRE].

[28] C. Cheung, L.J. Hall, D. Pinner and J.T. Ruderman, *Prospects and blind spots for neutralino dark matter*, *JHEP* **05** (2013) 100 [arXiv:1211.4873] [INSPIRE].

[29] ATLAS collaboration, *Search for direct production of the top squark in the all-hadronic ttbar + etmiss final state in $21\,fb^{-1}$ of p-pcollisions at $\sqrt{s} = 8$ TeV with the ATLAS detector*, ATLAS-CONF-2013-024 (2013).

[30] CMS collaboration, *Search for direct top squark pair production in events with a single isolated lepton, jets and missing transverse energy at $\sqrt{s} = 8\,TeV$*, CMS-PAS-SUS-12-023 (2012).

[31] Z. Han, A. Katz, D. Krohn and M. Reece, *(Light) stop signs*, *JHEP* **08** (2012) 083 [arXiv:1205.5808] [INSPIRE].

[32] D.S. Alves, M.R. Buckley, P.J. Fox, J.D. Lykken and C.-T. Yu, *Stops and MET: The shape of things to come*, *Phys. Rev.* **D 87** (2013) 035016 [arXiv:1205.5805] [INSPIRE].

[33] C. Kilic and B. Tweedie, *Cornering light stops with dileptonic m_{T2}*, *JHEP* **04** (2013) 110 [arXiv:1211.6106] [INSPIRE].

[34] M. Blanke, G.F. Giudice, P. Paradisi, G. Perez and J. Zupan, *Flavoured naturalness*, *JHEP* **06** (2013) 022 [arXiv:1302.7232] [INSPIRE].

[35] Y. Kats and D. Shih, *Light stop NLSPs at the Tevatron and LHC*, *JHEP* **08** (2011) 049 [arXiv:1106.0030] [INSPIRE].

[36] T. Han, K.-i. Hikasa, J.M. Yang and X.-m. Zhang, *The FCNC top squark decay as a probe of squark mixing*, *Phys. Rev.* **D 70** (2004) 055001 [hep-ph/0312129] [INSPIRE].

[37] M. Carena, A. Freitas and C. Wagner, *Light stop searches at the LHC in events with one hard photon or jet and missing energy*, *JHEP* **10** (2008) 109 [arXiv:0808.2298] [INSPIRE].

[38] M. Muhlleitner and E. Popenda, *Light stop decay in the MSSM with minimal flavour violation*, *JHEP* **04** (2011) 095 [arXiv:1102.5712] [INSPIRE].

[39] D0 collaboration, V. Abazov et al., *Search for the lightest scalar top quark in events with two leptons in $p\bar{p}$ collisions at $\sqrt{s} = 1.96\,TeV$*, *Phys. Lett.* **B 659** (2008) 500 [arXiv:0707.2864] [INSPIRE].

[40] CDF collaboration, T. Aaltonen et al., *Search for scalar top quark production in $p\bar{p}$ collisions at $\sqrt{s} = 1.96\,TeV$*, *JHEP* **10** (2012) 158 [arXiv:1203.4171] [INSPIRE].

[41] ATLAS collaboration, *Search for a supersymmetric top-quark partner in final states with two leptons in $\sqrt{s} = 8\,TeV$ pp collisions using $13\,fb^{-1}$ of ATLAS data*, ATLAS-CONF-2012-167 (2012).

[42] OPAL collaboration, G. Abbiendi et al., *Search for scalar top and scalar bottom quarks at LEP*, *Phys. Lett.* **B 545** (2002) 272 [*Erratum ibid.* **B 548** (2002) 258] [hep-ex/0209026] [INSPIRE].

[43] K. Krizka, A. Kumar and D.E. Morrissey, *Very light scalar top quarks at the LHC*, *Phys. Rev.* **D 87** (2013) 095016 [arXiv:1212.4856] [INSPIRE].

[44] A. Delgado, G.F. Giudice, G. Isidori, M. Pierini and A. Strumia, *The light stop window*, *Eur. Phys. J.* **C 73** (2013) 2370 [arXiv:1212.6847] [INSPIRE].

[45] H. Dreiner, M. Krämer and J. Tattersall, *Exploring QCD uncertainties when setting limits on compressed supersymmetric spectra*, *Phys. Rev.* **D 87** (2013) 035006 [arXiv:1211.4981] [INSPIRE].

[46] H.K. Dreiner, M. Krämer and J. Tattersall, *How low can SUSY go? Matching, monojets and compressed spectra*, *Europhys. Lett.* **99** (2012) 61001 [arXiv:1207.1613] [INSPIRE].

[47] Z.-H. Yu, X.-J. Bi, Q.-S. Yan and P.-F. Yin, *Detecting light stop pairs in coannihilation scenarios at the LHC*, *Phys. Rev.* **D 87** (2013) 055007 [arXiv:1211.2997] [INSPIRE].

[48] A. Choudhury and A. Datta, *New limits on top squark NLSP from LHC $4.7\,fb^{-1}$ data*, *Mod. Phys. Lett.* **A 27** (2012) 1250188 [arXiv:1207.1846] [INSPIRE].

[49] ATLAS collaboration, *Search for new phenomena in monojet plus missing transverse momentum final states using* 1 fb^{-1} *of pp collisions at* $\sqrt{s} = 7$ *TeV with the ATLAS detector*, ATLAS-CONF-2011-096 (2011).

[50] CMS collaboration, *Search for dark matter and large extra dimensions in monojet events in pp collisions at* $\sqrt{s} = 7$ *TeV*, *JHEP* **09** (2012) 094 [arXiv:1206.5663] [inSPIRE].

[51] J. Alwall, M. Herquet, F. Maltoni, O. Mattelaer and T. Stelzer, *MadGraph 5: going beyond*, *JHEP* **06** (2011) 128 [arXiv:1106.0522] [inSPIRE].

[52] T. Sjöstrand, S. Mrenna and P.Z. Skands, *PYTHIA 6.4 physics and manual*, *JHEP* **05** (2006) 026 [hep-ph/0603175] [inSPIRE].

[53] J. Conway et al., *PGS 4: Pretty Good Simulation of high energy collisions* (2006), webpage.

[54] R. Mahbubani, M. Papucci, G. Perez, J.T. Ruderman and A. Weiler, *Light nondegenerate squarks at the LHC*, *Phys. Rev. Lett.* **110** (2013) 151804 [arXiv:1212.3328] [inSPIRE].

[55] CMS collaboration, *Search for new physics in the multijet and missing transverse momentum final state in proton-proton collisions at* $\sqrt{s} = 7$ *TeV*, *Phys. Rev. Lett.* **109** (2012) 171803 [arXiv:1207.1898] [inSPIRE].

[56] ATLAS collaboration, *Search for direct sbottom production in event with two b-jets using* 12.8 fb^{-1} *of pp collisions at* $\sqrt{s} = 8$ *TeV with the ATLAS detector*, ATLAS-CONF-2012-165 (2012).

[57] CMS collaboration, *Inclusive search for supersymmetry using the razor variables in pp collisions at* $\sqrt{s} = 7$ *TeV*, *Phys. Rev. Lett.* **111** (2013) 081802 [arXiv:1212.6961] [inSPIRE].

[58] CMS collaboration, *A search for the decays of a new heavy particle in multijet events with the razor variables at CMS in pp collisions at* $\sqrt{s} = 7$ *TeV*, (2012)

[59] CMS collaboration, *Search for supersymmetry with the razor variables at CMS*, CMS-PAS-SUS-11-008 (2012).

[60] CMS collaboration, *Search for supersymmetry in final states with missing transverse energy and* 0, 1, 2, *or at least* 3 *b-quark jets in* 7 *TeV pp collisions using the variable alphaT*, *JHEP* **01** (2013) 077 [arXiv:1210.8115] [inSPIRE].

[61] L. Randall and D. Tucker-Smith, *Dijet searches for supersymmetry at the LHC*, *Phys. Rev. Lett.* **101** (2008) 221803 [arXiv:0806.1049] [inSPIRE].

[62] T. Junk, *Confidence level computation for combining searches with small statistics*, *Nucl. Instrum. Meth.* **A 434** (1999) 435 [hep-ex/9902006] [inSPIRE].

[63] A.L. Read, *Presentation of search results: the CL_s technique*, *J. Phys.* **G 28** (2002) 2693 [inSPIRE].

[64] W. Beenakker, R. Hopker and M. Spira, *PROSPINO: a program for the production of supersymmetric particles in next-to-leading order QCD*, hep-ph/9611232 [inSPIRE].

[65] P.J. Fox, R. Harnik, R. Primulando and C.-T. Yu, *Taking a razor to dark matter parameter space at the LHC*, *Phys. Rev.* **D 86** (2012) 015010 [arXiv:1203.1662] [inSPIRE].

[66] CMS collaboration, *Search for supersymmetry in all-hadronic events with* α_t, CMS-PAS-SUS-11-003 (2011).

[67] CMS collaboration, *A search for the decays of a new heavy particle in multijet events with the razor variables at CMS in pp collisions at* $\sqrt{s} = 7$ *TeV*, CMS-PAS-SUS-12-009 (2012).

[68] *Reproducing the razor limit in your SUSY study*, webpage.